

# New journal of chemistry

## *Supplementary materials*

*for*

### **The synthesis of 1,6-disubstituted pyrene-based conjugated microporous polymers for reversible adsorbing and fluorescent sensing iodine**

Tong-Mou Geng<sup>a\*</sup>, Can Zhang<sup>a</sup>, Chen Hu<sup>a</sup>, Min Liu<sup>a</sup>, Ya-Ting Fei<sup>a</sup>, and Hong-Yu Xia<sup>a</sup>

*a AnHui Province Key Laboratory of Optoelectronic and Magnetism Functional Materials;*

*School of Chemistry and Chemical Engineering, Anqing Normal University, Anqing 246011,*

*China*

#### **Corresponding Author:**

Tongmou Geng

Mailing Address: School of Chemistry and Chemical Engineering, Anqing Normal University,  
Anqing 246011, China

E-mail addresses: gengtongmou@aqnu.edu.cn (TM Geng).

## **Experimental Section**

### *S1. Materials*

1,6-Dibromopyrene was purchased Fluorochem. Ltd. 4-Cyanophenylboronic acid (98%), diphenylamine, 4-(diphenylamino)phenylboronic acid (DPAPB, 98 %), and sodium tert-butoxide (99 %) were bought J &K scientific LTD.; Tetrakis(-triphenylphosphine) palladium ( $\text{Pd}(\text{PPh}_3)_4$ ), copper(I) iodide ( $\text{CuI}$ ) ( $\geq 99.5\%$ ), and trifluoromethanesulfonic acid (TFMSA, 98%), methanesulfonic acid (MSA), o-dichlorobenzene, and 2,4,6-trichloro-1,3,5-triazine (TCT, cyanuric chloride, CC) were purchased from Aladdin chemistry Co. Ltd.; 1,3,5-Triethylbenzene (TEB,  $>98\%$ ) was purchased from Tokyo Chemical Industry Co. Ltd. Iodine, triethylamine (TEA), N,N-dimethylformamide (DMF, 99.0%), 1,4-dioxane, ethanol (EtOH), tetrahydrofunan (THF), chloroform, acetone, anhydrous sodium sulfate, o-nitrophenol (o-NP), picric acid (PA), 4-nitrotoluene (p-NT), phenol (PhOH), dinitrotoluene (DNT), 1,4-dinitrobenzene (p-DNB), 1,3-dinitrobenzene (m-DNB), and sodium carbonate were obtained commercially, and used without further purification.

### *Methods*

### *S2. Characterization*

The infrared spectra were recorded from 400 to 4000  $\text{cm}^{-1}$  on an iS50FT-IR spectrometer by using KBr pellets. Solid-state  $^{13}\text{C}$  CP/MAS NMR measurements were recorded on a Bruker AVANCE III 400 WB spectrometer at a MAS rate of 5 kHz and a CPcontact time of 2 ms. Elemental analyses were carried out on a VARIO ELIII cube analyzer. UV–Vis spectra were recorded on an UV-2501PC spectrometer.

Scanning electron microscopy was performed on a S-3400N microscope. X-ray diffraction data were recorded on a XRD600 diffractometer by depositing powder on glass substrate, from  $2\theta = 5^\circ$  up to  $90^\circ$  with  $0.02^\circ$  increment. Thermogravimetric analysis (TGA) measurements were performed on a CDR-4P TGA under  $N_2$ , by heating to  $800\text{ }^\circ\text{C}$  at a rate of  $10\text{ }^\circ\text{C min}^{-1}$ . The Brunauer-Emmett-Teller (BET) method was utilized to calculate the specific surface areas and pore volume, the Saito-Foley (SF) method was applied for the estimation of pore size distribution. Raman spectra were acquired using a DXR equipped with a 532 nm diode laser. Fluorescence spectra were recorded on a F-4500 and FL750 spectrophotometer. The samples were prepared as follows: dried CMPs powder (10 mg) ground with an agate mortar was added to 10 mL of organic solvents. After the resulting mixture was well dispersed with ultrasound, the dispersion colloid was obtained. Time-resolved fluorescence spectroscopy was recorded on steady state/transient fluorescence spectrometer.

### *S3. Synthesis of the monomer 1,6-di(4-cyanophenyl)pyrene (CPP)*

$Pd(PPh_3)_4$  (0.2000 g, 0.1778 mmol) was added to a well degassed solution of 1,6-dibromopyrene (1.4419 g, 4.0 mmol), 4-cyanophenylboronic acid (1.7633 g, 12.0 mmol),  $K_2CO_3$  (1.4022 g, 13.23 mmol), DMF (71.43 mL), and  $H_2O$  (5.71 mL). The resulting mixture was stirred at  $100\text{ }^\circ\text{C}$  for 72 h under argon atmosphere. After cooling down at room temperature, the mixture was extracted with chloroform for three times ( $3 \times 30$  mL). The organic phase was then washed with water ( $3 \times 30$  mL) and dried with anhydrous magnesium sulfate overnight, filtered and evaporated to dryness. The crude product was purified by column chromatography (Silica Gel,  $CHCl_3$ ). Further

purification of the product was carried out by recrystallization from  $\text{CH}_2\text{Cl}_2$  afforded CPP (0.5207 g) in 61.18 % yield as a khaki powder.  $^1\text{H-NMR}$  (400 MHz,  $\text{CDCl}_3$ ): 8.27-8.20, 8.13-8.12, 7.81-7.98, 7.78-7.68, 7.56-7.46. FTIR (KBr,  $\text{cm}^{-1}$ ): 2226, 1675, 1606, 1489, 1438, 1192, 1119, 809, 722, 541. Elemental analysis: Anal. calc. for  $\text{C}_{30}\text{H}_{16}\text{N}_2$ : 404.47, C 89.08, H 3.987, N 6.926; found: C 89.56, H 4.210, N 6.606.

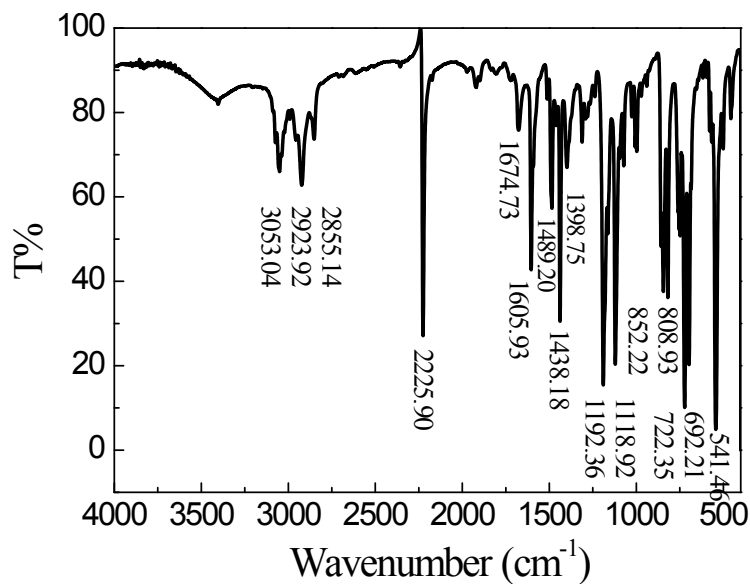


**Fig. S1.** The FT-IR spectrum of the monomer CPP.

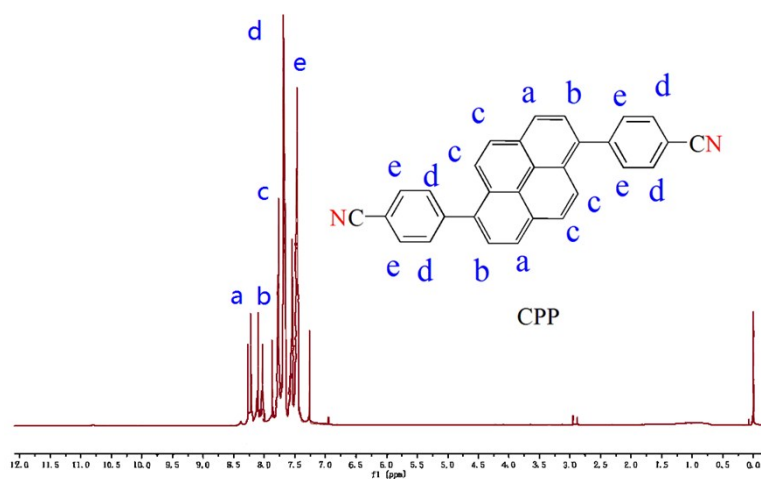


**Fig. S2.** The  $^1\text{H}$  NMR spectrum of the monomer CPP.

S4. *Synthesis of the monomer N,N,N',N'-tetrapheny-1,6- (diazyl) pyrene (TPDP)*

A single-necked 100 mL round-bottom flask was charged with diphenylamine (1.3552 g, 8 mmol), sodium tert-butoxide (1.1532 g, 12 mmol), tetrakis(triphenylphosphine)palladium(0) (0.2311 g, 0.20 mmol), dry toluene (12 mL), 1,6-dibromopyrene (1.4402 g, 4 mmol), which was heated at 110 °C for 24 h under a nitrogen atmosphere. After cooling to room temperature, the reaction mixture was quenched with water and extracted with dichloromethane (6×25 mL). The combined organic solution was washed with water and dried over anhydrous Na<sub>2</sub>SO<sub>4</sub>. Evaporation of volatiles left a atrovirens solid, which was separated by silica gel column chromatography, by using petroleum ether/dichloromethane (v/v = 1:1) as eluent, affording monomer TPDP in 85.76 % yield as an orange red solid. FT-IR (cm<sup>-1</sup>): 1587, 1485, 11261, 845, 744, 691. <sup>1</sup>H NMR (400 MHz, CDCl<sub>3</sub>): δ (ppm) 7.25, 7.25, 7.20; 7.08, 7.06, 7.01, 7.00; 6.98-6.85. Elemental analysis of TPDP: Calculated value (%): C (89.52), H (5.26), N (5.22); Found (%): C (89.65), H (4.881), N (5.473).

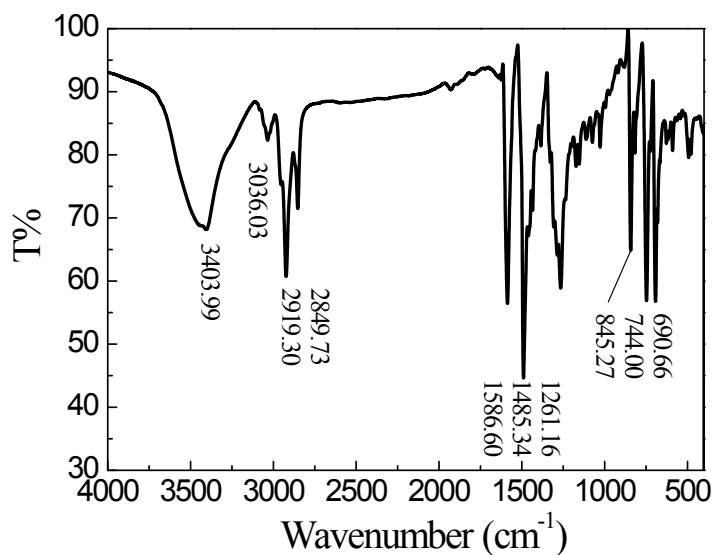


**Fig. S3.** The FT-IR spectrum of the monomer TPDP.

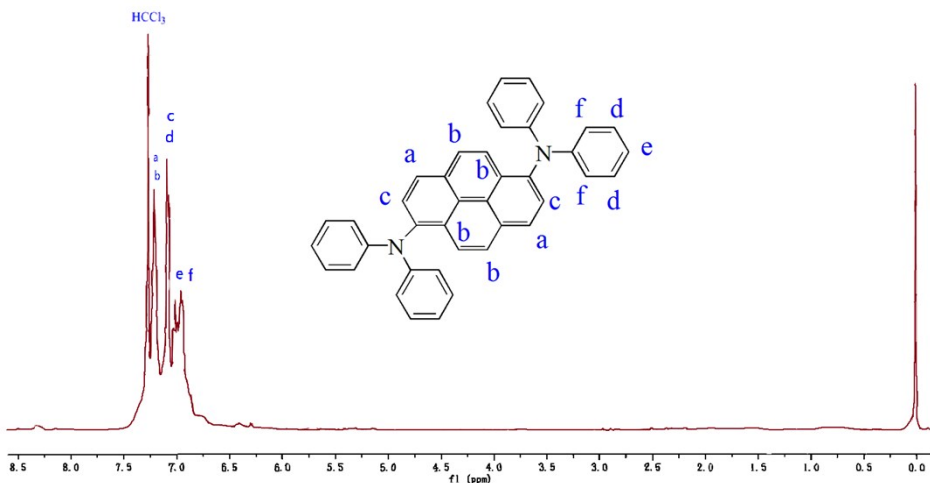


**Fig. S4.** The <sup>1</sup>H NMR spectrum of the monomer TPDP.

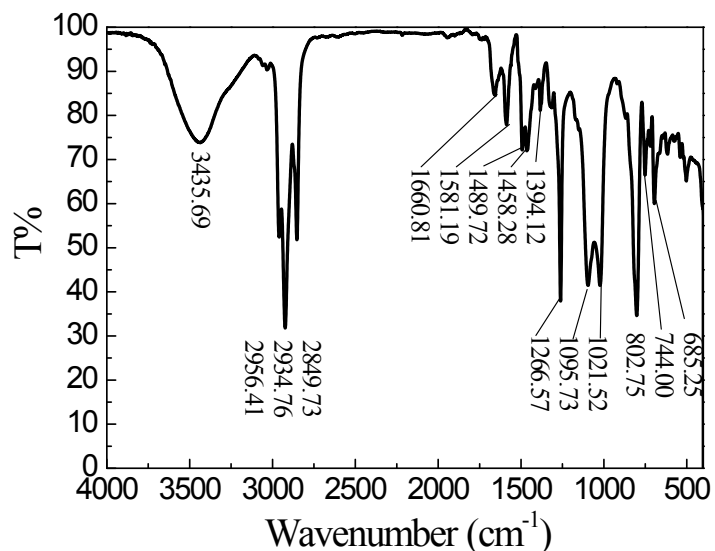
*S5. Synthesis of the monomer di(triphenylamine-ly)1,6-pyrene (DTPAP)*

A mixture of 1,6-dibromopyrene (1.0802 g, 3 mmol), 4-(diphenylamino)phenylboronic acid (6.0 mmol, 1.7348 g), and tetrakis(triphenylphosphine)palladium(0) (0.0857 mmol, 100 mg) were added into a 100-mL flask. Sodium carbonate (6.6143 mmol, 0.7011 g) was dissolved in 3 mL water and then the solution was added to the 100-mL flask. Dimethylformamide (36 mL) was added to the above flask, and the solution was refluxed at 110 °C for 72 h under N<sub>2</sub>. After cooling down at room temperature, the mixture was evaporated and the resulted solid was extracted with chloroform for three times (3×30 mL). The organic phase was then washed with water (3×30 mL) and dried with anhydrous magnesium sulfate overnight. The final yellow powder product was obtained via purification using silica column chromatography with petroleum ether/dichloromethane (v/v = 1:1) as eluent. The yield was 71.48 %. FT-IR (cm<sup>-1</sup>): 1661, 1581, 1490, 1458, 1394, 1267, 1096, 1022, 803, 744, and 685. <sup>1</sup>H NMR

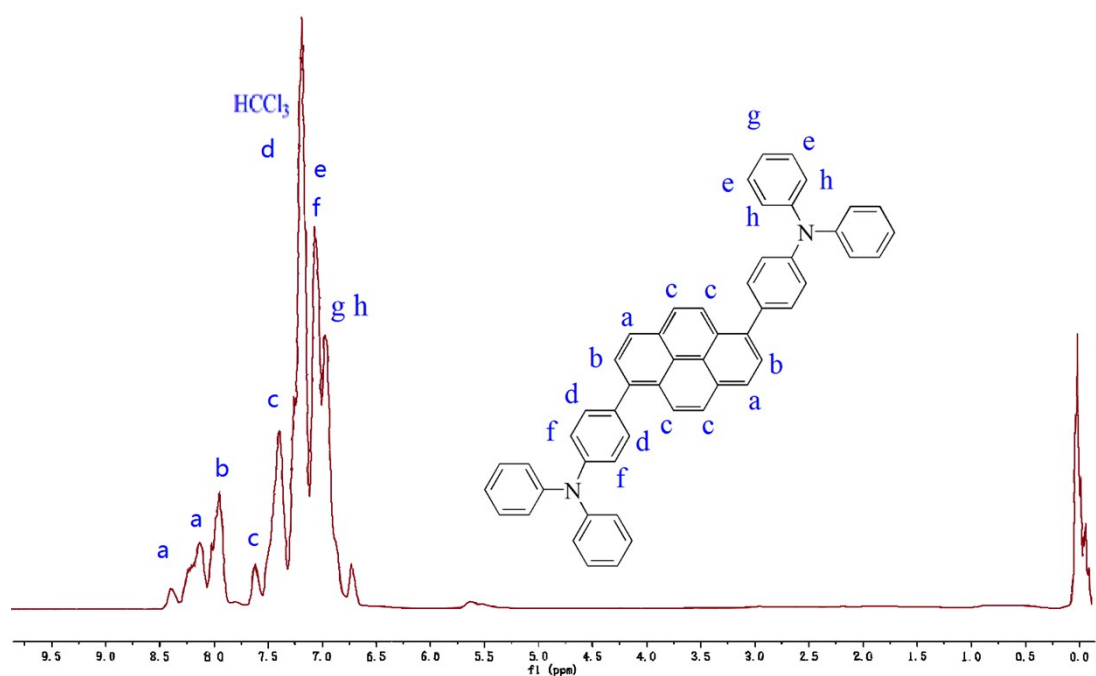
(400 MHz, CDCl<sub>3</sub>): δ (ppm) 8.37, 8.15, 7.94; 7.60, 7.37; 7.17; 7.05-7.02; 6.98-6.71.

Elemental analysis of DTPAP: Calculated value (%): C (90.96), H (5.27), N (4.07);

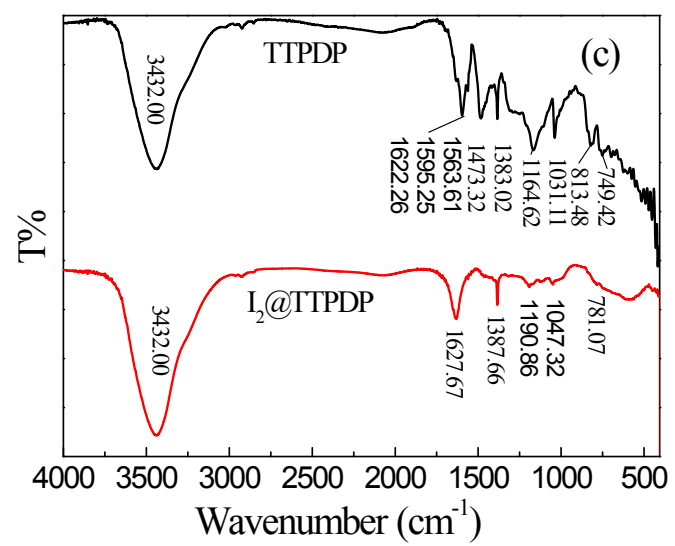
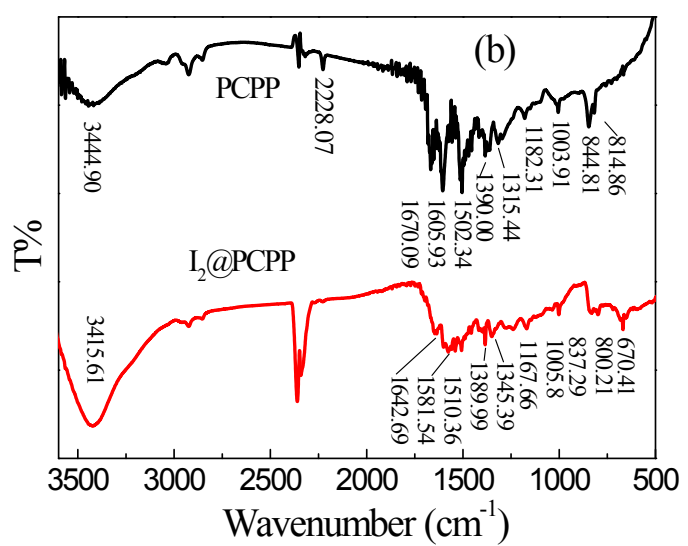
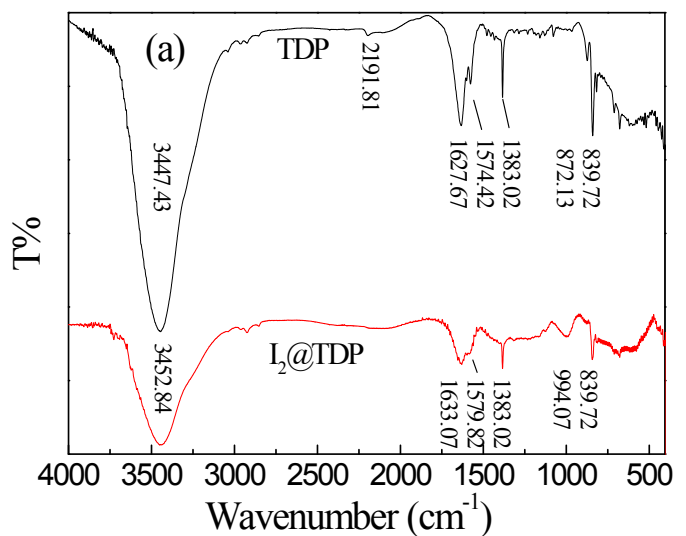
Found (%): C (90.84), H (4.975), N (4.186).

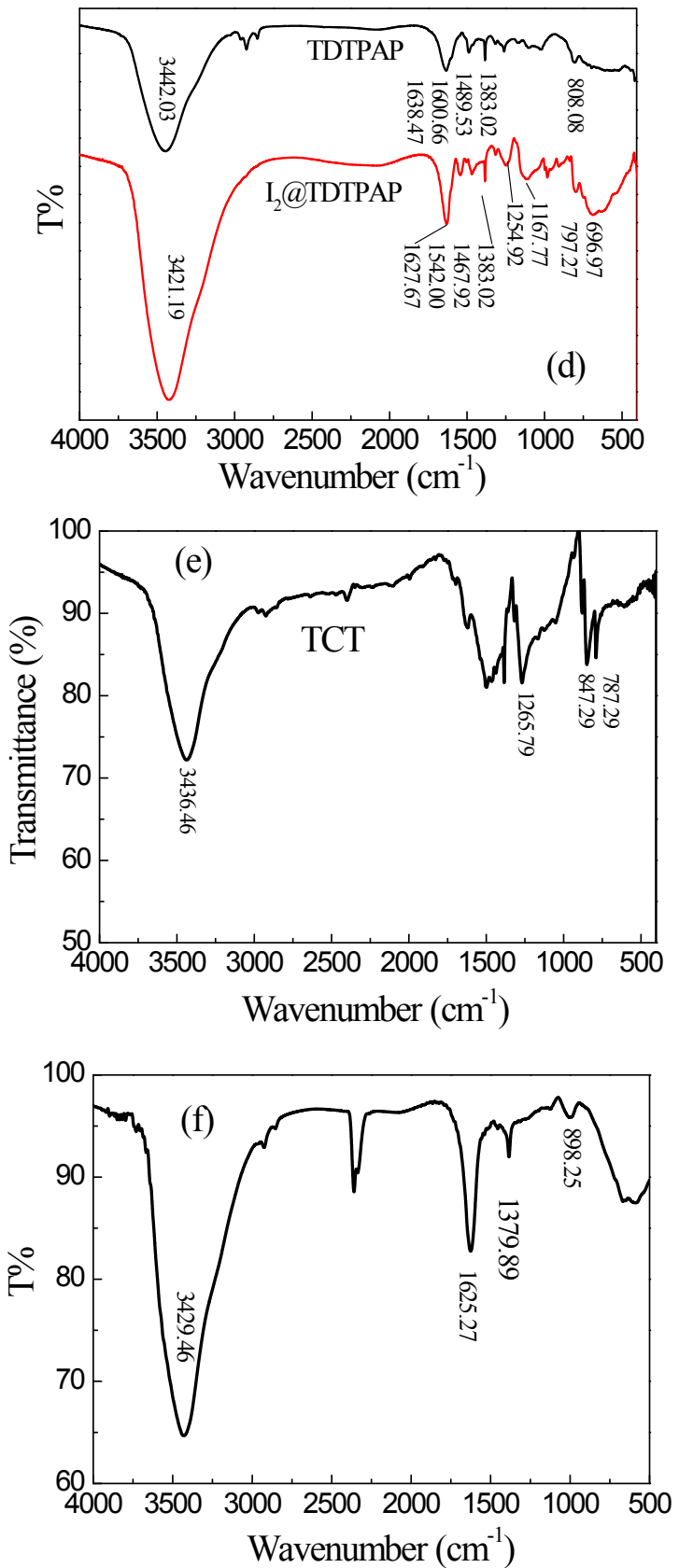


**Fig. S5.** The FT-IR spectrum of the monomer DTPAP.

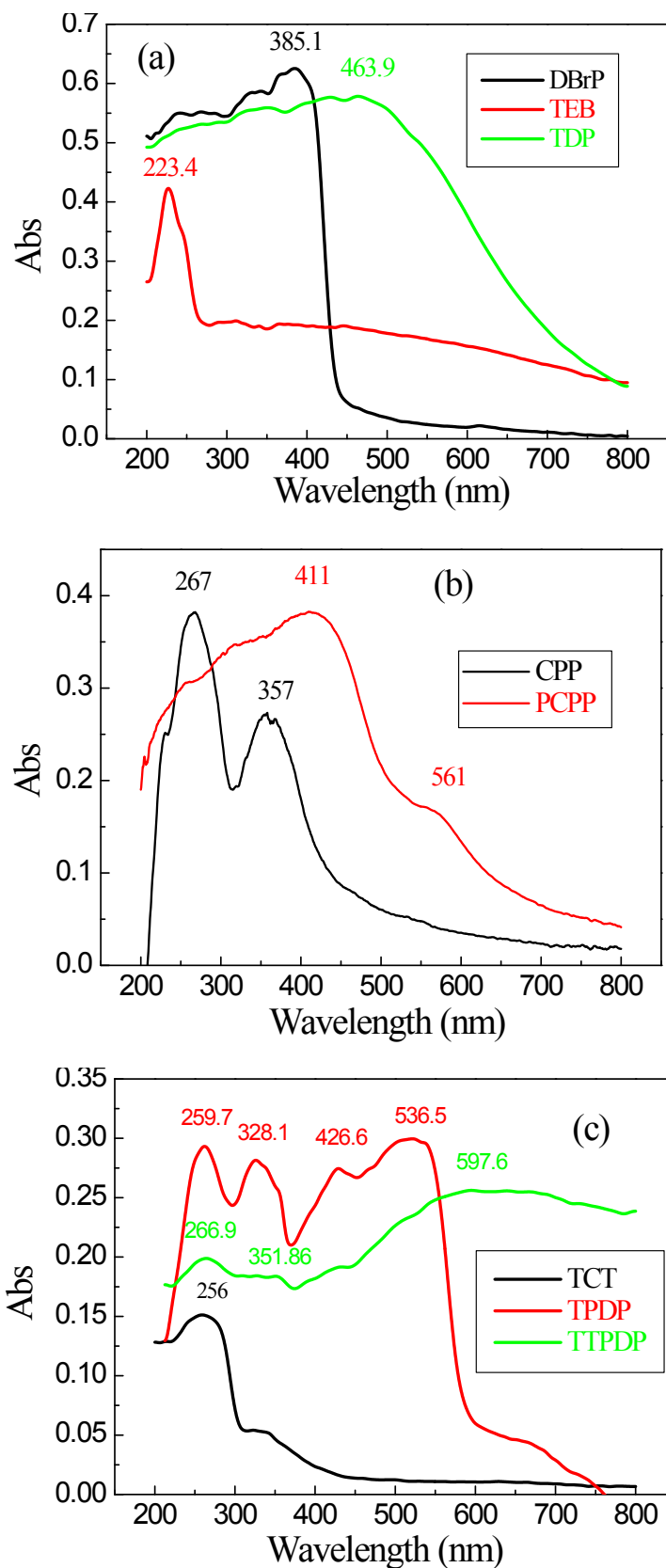


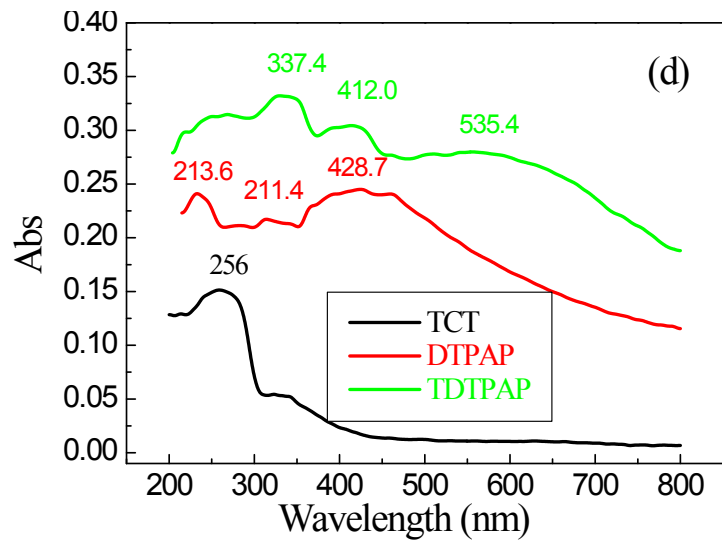
**Fig. S6.** The <sup>1</sup>H NMR spectrum of the monomer DTPAP.



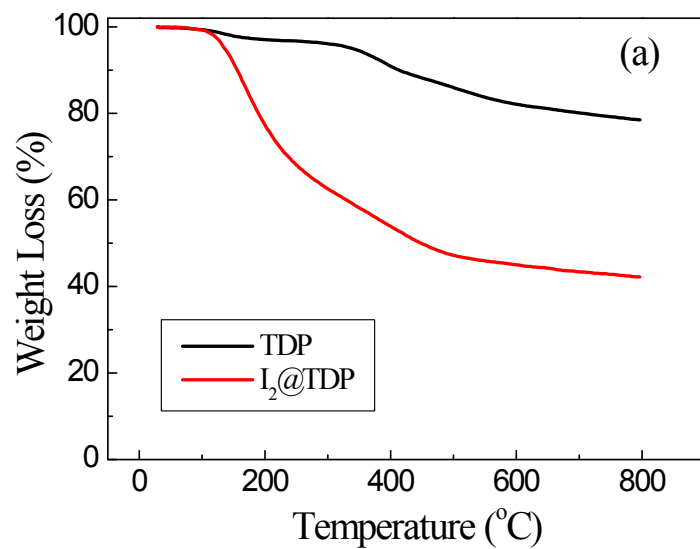


**Fig. S7.** The FT-IR spectra of the (a) TDP,  $\text{I}_2@\text{TDP}$ , (b) PCPP,  $\text{I}_2@\text{PCPP}$ , (c) TPPDP,  $\text{I}_2@\text{TPPDP}$ , (d) TDTPAP,  $\text{I}_2@\text{TDTPAP}$ , (e) TCT, and (f)  $\text{I}_2$ .





**Fig. S8.** UV-Vis spectra of monomers and CMPs. (a) TDP, (b) PCPP, (c), TTPDP, and (d) TDTPAP.



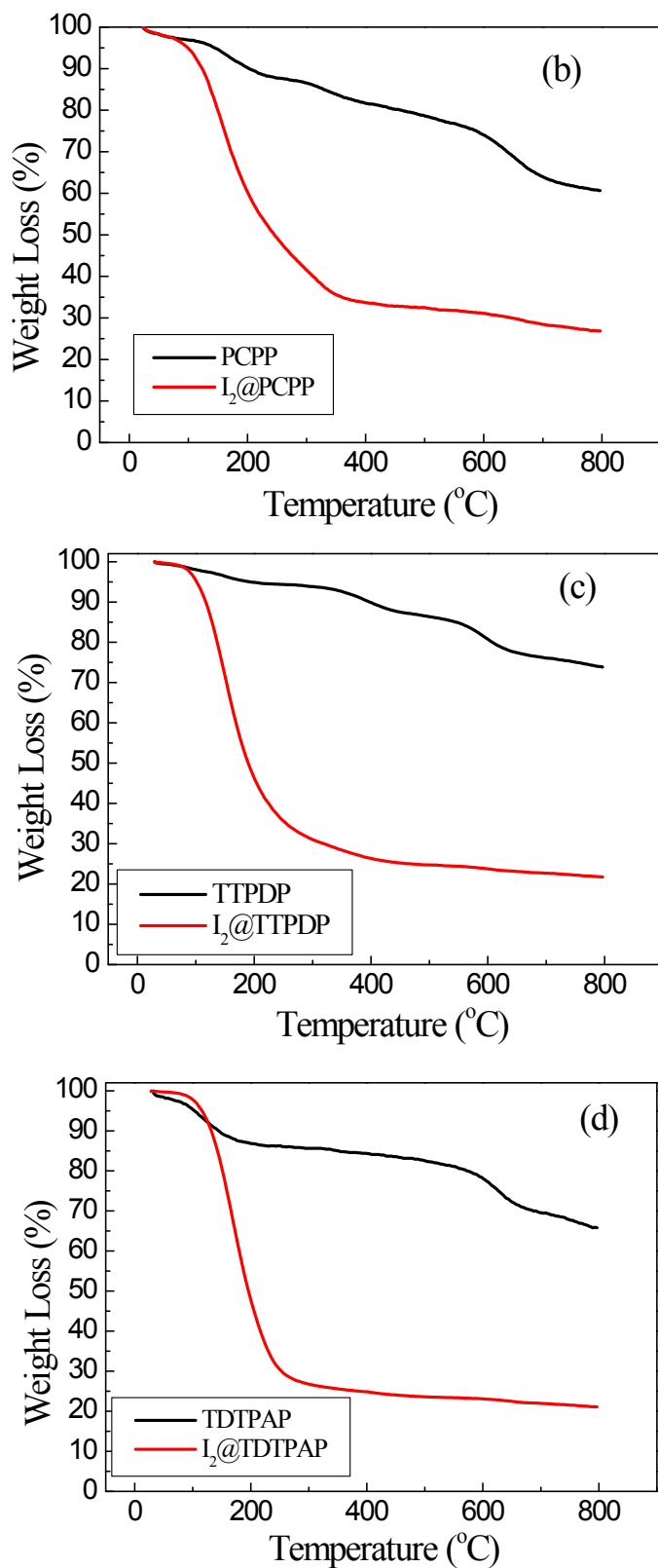


**Fig. S9.** Thermogravimetric analysis of CMPs and  $I_2$ @CMPs under  $N_2$ . (a) TDP, (b) PCPP, (c) TTPDP, and (d) TDTPAP.

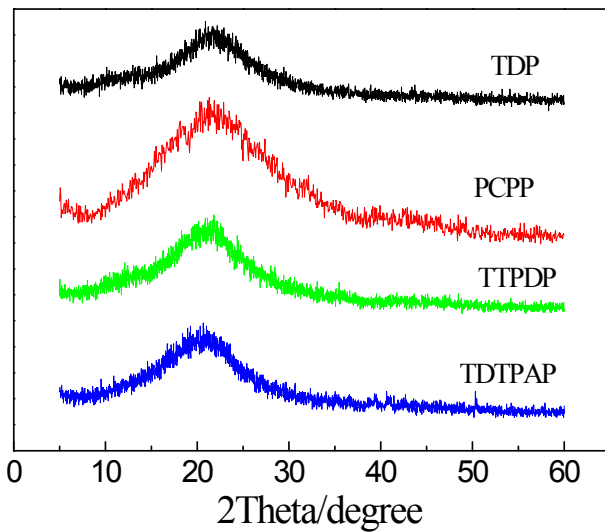


**Fig. S10.** XRD patterns for TDP, PCPP, TTPDP, and TDTPAP.

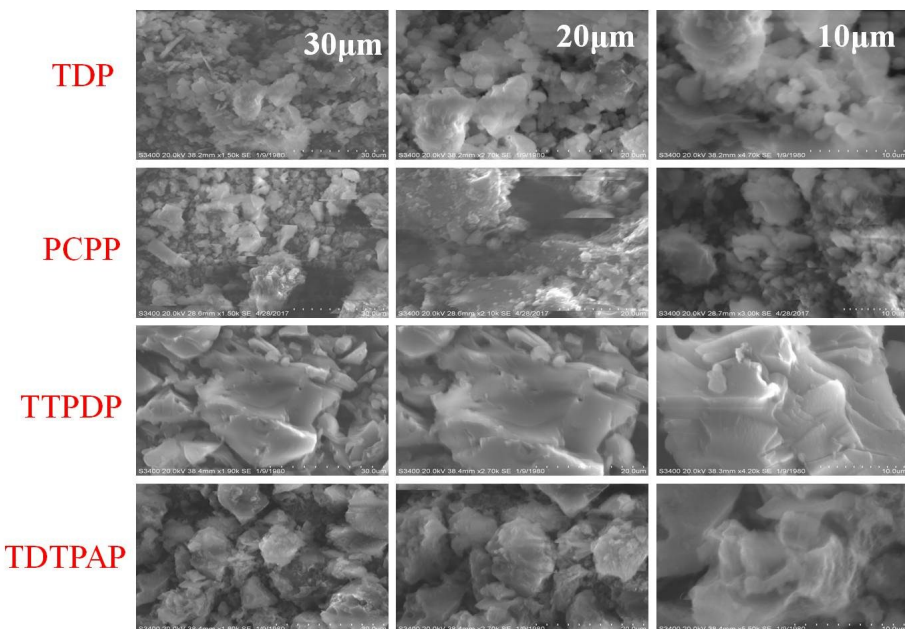


**Fig. S11.** The SEM images of TDP, PCPP, TTPDP, and TDTPAP.

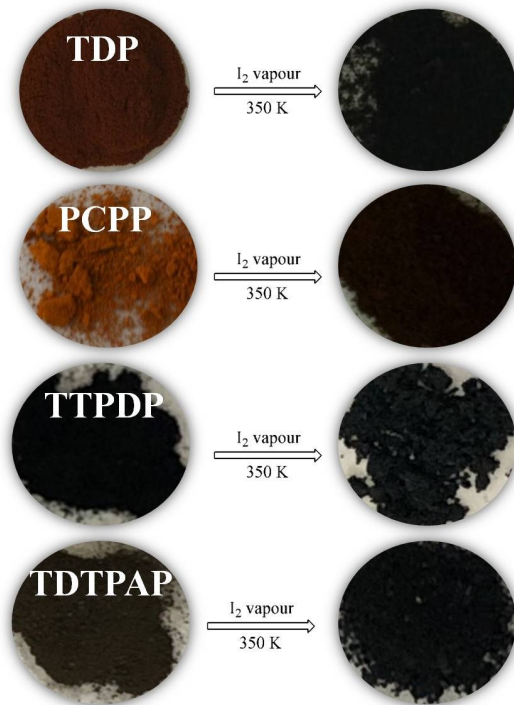


**Fig. S12.** Photographs showing the colour changes before and after iodine capture for TDP, PCPP, TTPDP, and TDTPAP.

**Table S 1.** Summary of surface area and iodine sorption properties of pyrene-based CMPs.

Sample	BET (m <sup>2</sup> g <sup>-1</sup> )	T (°C)	Iodine uptake (g g <sup>-1</sup> )	Refs
Por-Py-CMP	1014	77	1.30	[14] <i>RSC Adv.</i> 6 (2016) 75478–75481.
CalP4	759,	75	2.20,	[18] <i>Chem. Mater.</i> 21 (2017)
CalP4-Li	445		3.12	8968–8972
CONs,	153,	40	1.20,	[19] <i>ChemNanoMat.</i> 4 (2018)
COTs	35		0.60	61–65
PTThP-2,	370.8,	77	1.65	<i>J. Polym. Res.</i> 2019, 26: 113–122.
PTThP-3	748.2		2.00	
TDP	261.9,	77	0.61	<i>This work</i> .
PCPP	43.0,		3.07	
TTPDP	187.5,		3.49	
TDTPAP	695.2		4.19	

**Table S 2.** Summary of surface areas and iodine sorption properties of triazine-based CMPs and triphenylamine-based CMPs.

Type of CMPs	Sample	BET (m <sup>2</sup> g <sup>-1</sup> )	T (°C)	Iodine uptake (g g <sup>-1</sup> )	Refs
Triazine - based CMPs	NAPOP-1	657	75	2.06	<i>J. Polym. Sci., Part A: Polym. Chem.</i> 54 (2016) 1724–1730
	NAPOP-2	458		2.39	
	NAPOP-3	702		2.41	
	NAPOP-4	626		2.65	
	H <sub>C</sub> OF-1	-	75	2.9±0.1	<i>J. Am. Chem. Soc.</i> 139 (2017) 7172–7175.
	H <sub>C</sub> OFs2-4		75	3.5	<i>J. Am. Chem. Soc.</i> 141 (2019) 10915–10923
	TTPT	315.5	77	1.77	<i>Polym. Chem.</i> 9 (2018) 777–784.
	NT-POP@800-1-6	499, 630, 475, 736, 643, 712	77	0. 68, 1.92, 0.56, 1.49, 1.52, 0.95	<i>Scientific Reports</i> 8 (2018) 1867.
	NRPP-1	1579	80	1.92	<i>ACS Appl. Mater. Inter.</i>
	NRPP-2	1028		2.22	10 (2018) 16049–16058.
	PAN1, PAN2, PAN3, PAN4, PAN5	618, 542, 194, 522, 439	75	1.33, 2.45, 2.81, 2.37, 1.89	<i>J. Appl. Polym. Sci.</i> 15 (2018) 46106

TatPOP-2	50.5	75	4.50	<i>Chem. Commun.</i> 54 (2018) 8450–8453.
MelPOP-2	36.5		2.62	
CSU-CPOPs-2	554.8	75	4.24	<i>ACS Appl. Mater. Inter.</i> 30 (2019) 27335–27342.
CTF-Cl-1	516	77	2.68	<i>Chem. –Asian J.</i> 19 (2019) 3259–3263.
CTF-Cl-2	599		2.89	
CTF-Cl-3	590		2.85	
CTF-Cl-4	889		3.12	
N-HCP	222.8	75	2.57	<i>Sep. Purifi.n Technol.</i> 2019 116260.
CaCOP1	10.86	75	2.41	<i>Mater. Chem. Phys.</i> 239 (2020) 122328.
CaCOP2 CaCOP3	20.16 80.09		1.85 1.72	
TPT-DHBDXCOFs X=0, 25, 50, 75, 100*		75	5.43, 4.65, 4.30, 4.12, 3.88	<i>Chem. Mater.</i> 7 (2018) 2299-2308.
TTA-TTB COF*	1733	77	4.98	<i>Adv. Mater.</i> 2018, 1801991.
TPT-Azine-COF*	1020	75	2.19	<i>ACS Appl. Nano Mater.</i> 9 (2018) 4756–4761
TPT-TAPB-COF*	957		2.25	
TPT-DMB COF*	-	75	5.15	<i>Sci. China Chem.</i> 1 (2019) 207–214.

Triphenylamine - based CMPs	JUC-Z2	2081	25	1.44	<i>J. Mater. Chem. A</i> 2 (2014) 7179–7187.
	SIOC-COF-7	618	75	4.81	<i>Chem. Commun.</i> 53 (2017) 7266–7269.
	PTPATTh	594	77	3.13	<i>J. Solid State Chem.</i> 265 (2018) 85–91
	PTPATCz	894		2.56	
	CMP-LS4	462	80	3.32	<i>Polym. Chem.</i> 20 (2019)
	CMP-LS5	1185		4.40	2608–2615.
The CMPs Containing both triazine and triphenylamine units	CMP-LS6	679		2.44	
	TTPB	222.25	77	4.43	<i>J. Mater. Chem. A</i> 5 (2017) 7612–7617.
	TPPA	512.39	77	4.90	<i>J. Mater. Chem. A</i> 6 (2018) 2808–2816.
	TTDAB	1.643		3.13	
	TmMTDAB	2.778		3.04	
	TTPA	308	77	4.92	<i>Micropor. Mesopor. Mat.</i> 273 (2019) 163–170
The CMPs Containing both triazine and triphenylamine units	TTDATA	491		4.72	
	TTMDATA	456		4.49	
The CMPs Containing both triazine and triphenylamine units	TTTAT	564.8	77	3.41	<i>Micropor. Mesopor. Mat.</i> 284 (2019) 468–475 3.
	TTDAT	44.1		2.91	

	TS-TAD	828	77	4.15	<i>Eur. Polym. J.</i> 115 (2019) 37–44.
	TS-TADP	783		3.65	
	TDTPAPz	4.19	77	4.41	<i>Environ. Sci. Pollut. Res.</i>
	TTDPz	4.41		3.12	31 (2019) 1614–7499
	TDP	261.9,	77	0.61	<i>This work.</i>
	PCPP	43.0,		3.07	
	TTPDP	187.5,		3.49	
	TDTPAP	695.2		4.19	

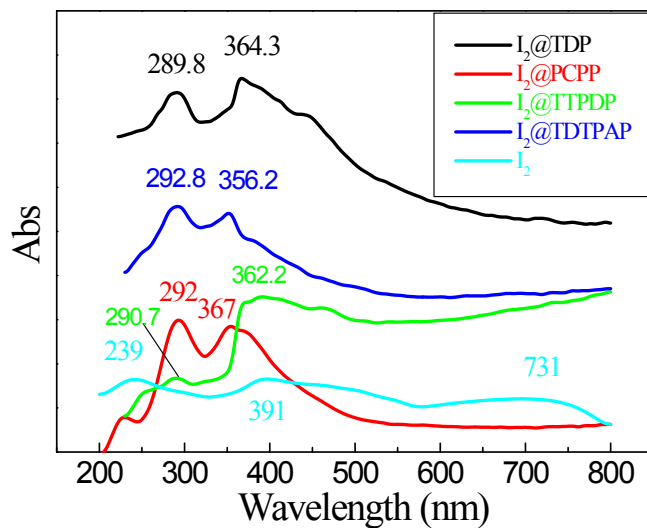
\*The triazine-based CMPs containing imino group from aldehyde-amine polycondensation reaction

**Table S3.** The peak shifts of FT-IR spectra of CMPs and I<sub>2</sub>@CMPs.

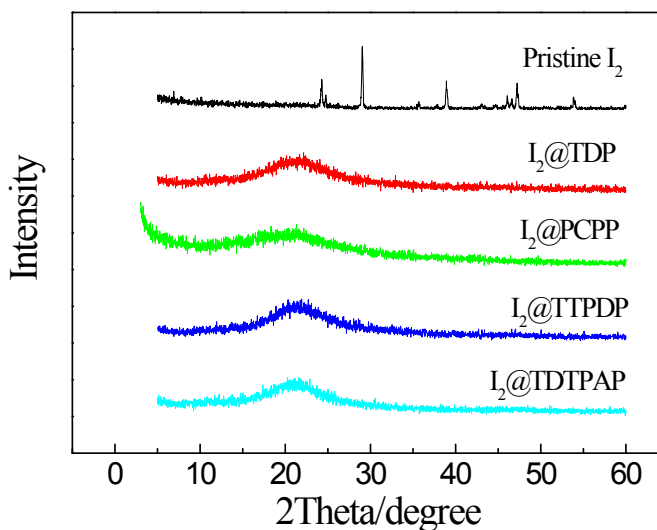
(a)	TDP	I <sub>2</sub> @TDP	shift
benzene ring	1574	1580	6
-C≡C-	2192	-	-
pyrene ring: in-plane	1628	1633	5
benzene ring: in-plane	1383	1383	0
benzene, pyrene ring: out-of-plane	840	840	0
H <sub>2</sub> O	3447	3453	6

(b)	PCPP	$I_2@PCPP$	shift
triazine ring: in-plane	1502	1510	8
benzene/triazine	1390/1315	1390/1345	0/30
pyrene ring: in-plane	1670	1642	-28
benzene ring: in-plane	1606	1582	-24
benzene, pyrene, triazine ring: out-of-plane	845/815	837/800	-8/-15
$H_2O$	3445	3416	-29
(c)	TTPDP	$I_2@TTPDP$	shift
triazine ring: in-plane	1564	-	-
benzene/triazine	1383/1473	1388/1388	5/-85
pyrene ring: in-plane	1622	1628	6
benzene ring: in-plane	1595	-	-
benzene, pyrene, triazine ring: out-of-plane	813	781	32
$H_2O$	3432	3432	0
(d)	TDTPAP	$I_2@TDTPAP$	shift
triazine ring: in-plane	1468	1490	22
benzene ring	1383	1383	0
pyrene ring: in-plane	1628	1638	10
benzene ring: in-plane	1542	1601	19
benzene, pyrene, triazine ring:	797	808	9

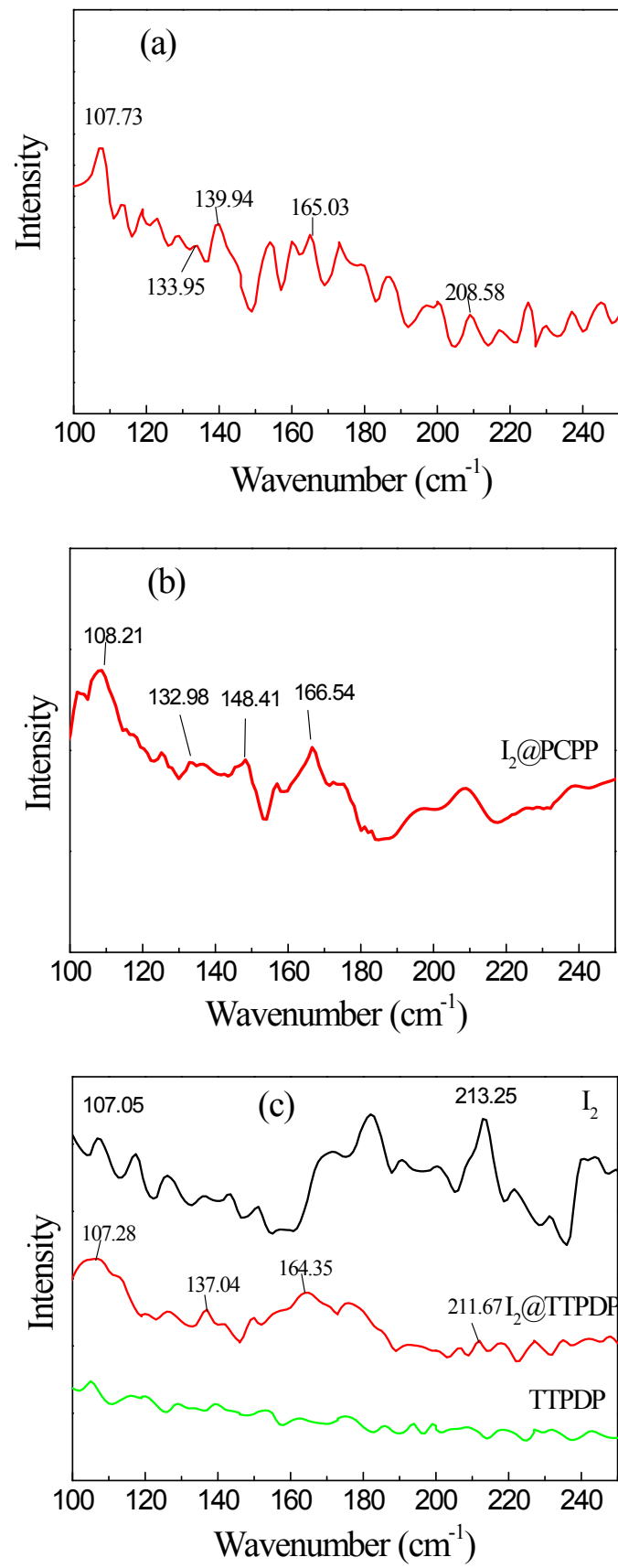
out-of-plane			
H <sub>2</sub> O	3421	3442	21

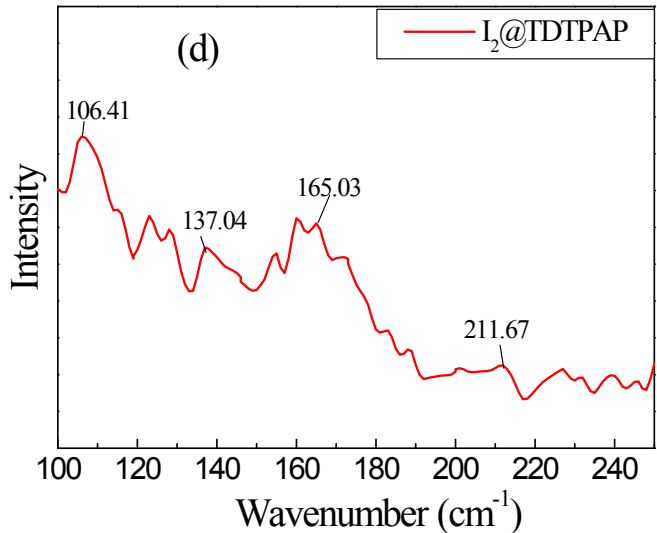


**Fig. S13.** UV-Vis spectra of monomers and iodine-loaded CMPs. I<sub>2</sub>@TDP, I<sub>2</sub>@PCPP, I<sub>2</sub>@TTPDP, I<sub>2</sub>@TDTPAP, and pristine I<sub>2</sub>.

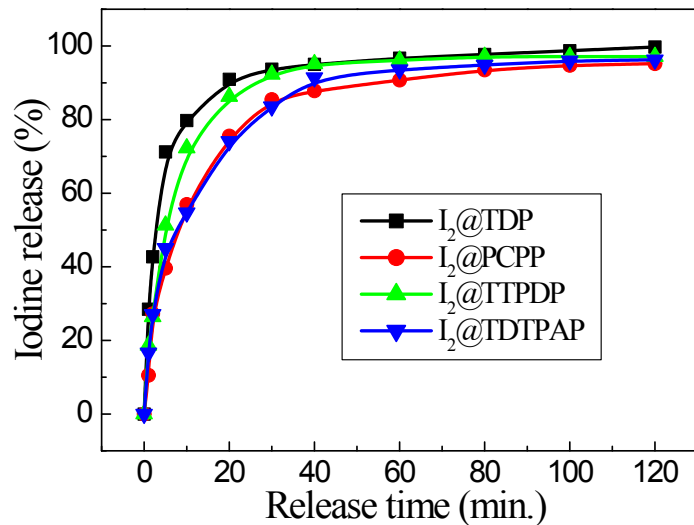


**Fig. S14.** XRD patterns for pristine I<sub>2</sub>, I<sub>2</sub>@TDP, I<sub>2</sub>@PCPP, I<sub>2</sub>@TTPDP, and I<sub>2</sub>@TDTPAP.

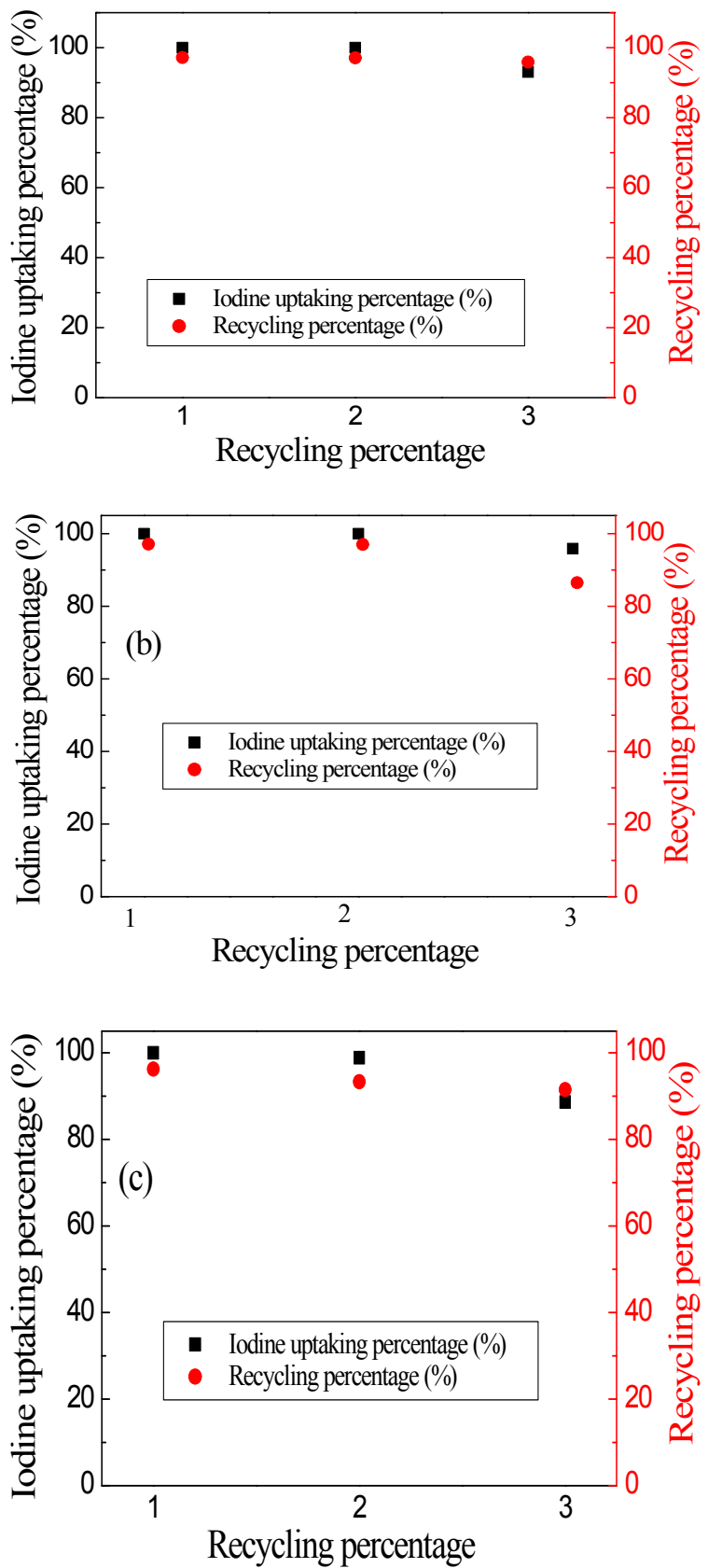




**Fig. S15.** Raman spectrum of iodine (black), iodine-loaded CMPs obtained by iodine vapor adsorption process (red) and CMPs (green). (a)  $I_2$ @TDP, (b)  $I_2$ @PCPP, (c)  $I_2$ @TTPDP, and (d)  $I_2$ @TDTPAP.

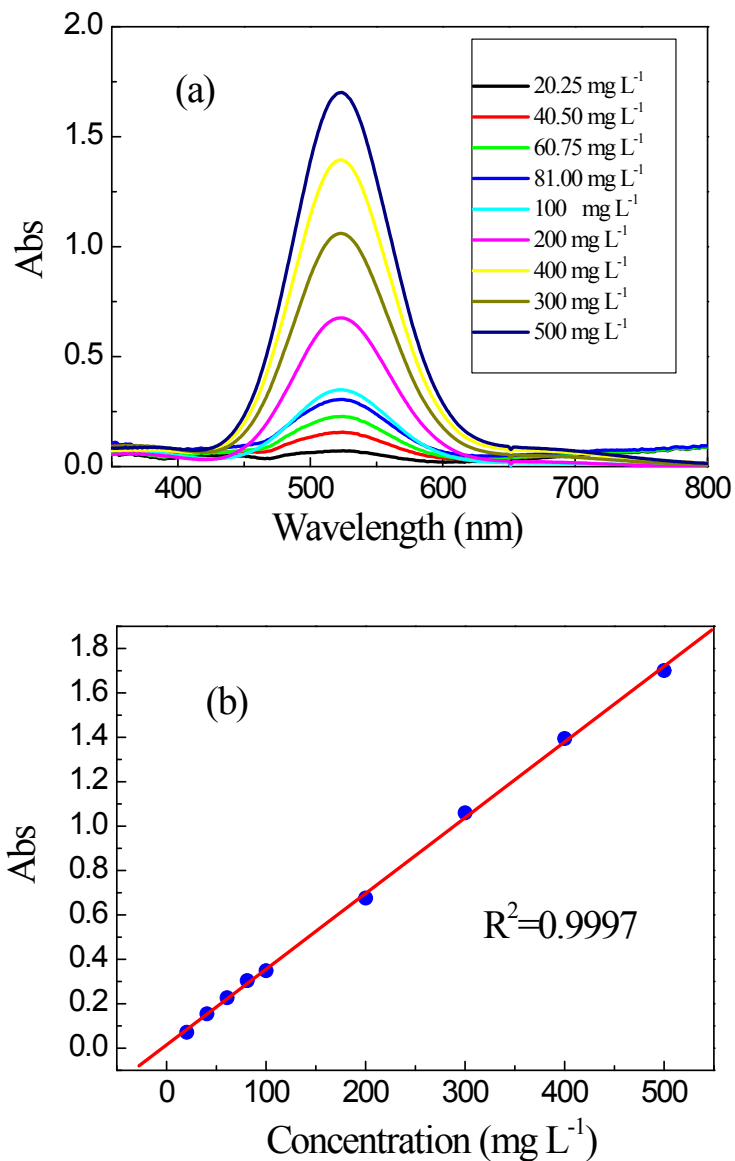


**Fig. S16.** Controlled release of iodine upon heating the loaded CMPs at 398 K.

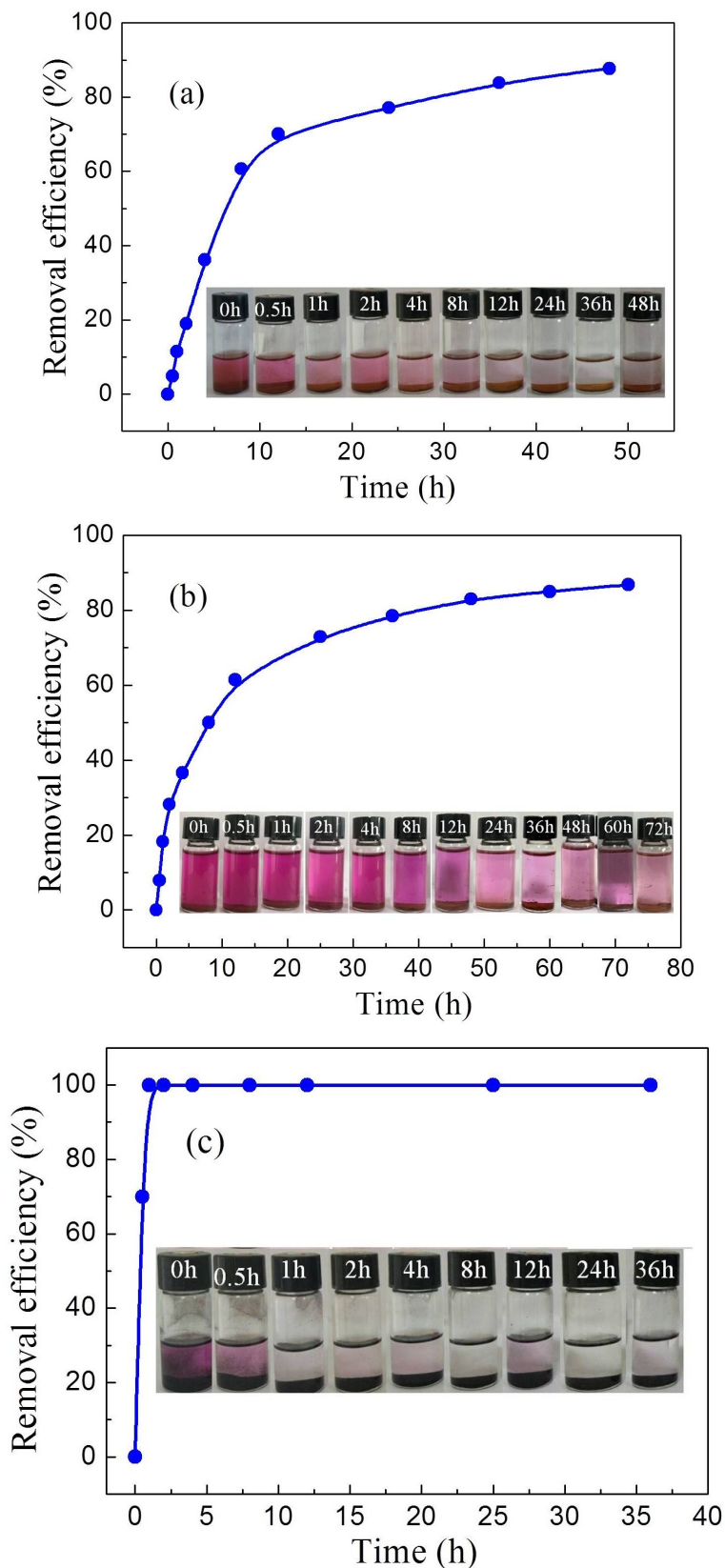


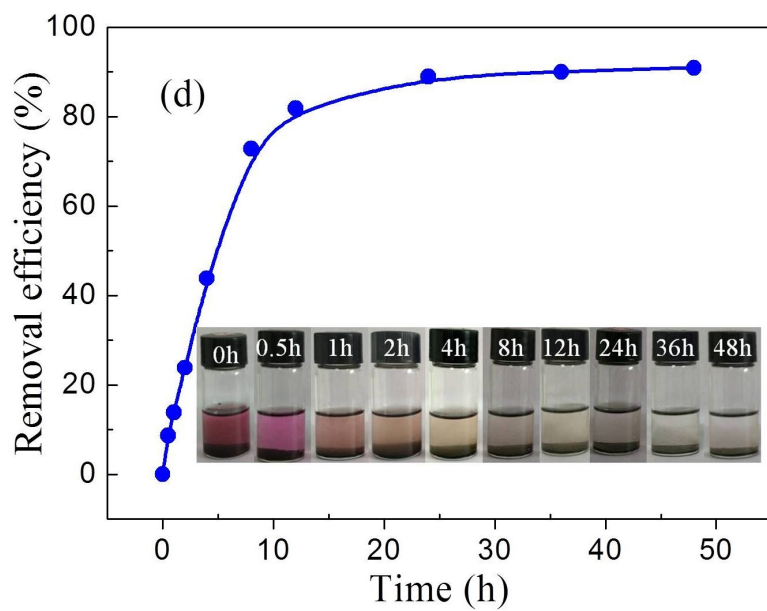
**Fig. S17.** Reusability of (a) PCPP, (b) TTPDP, and (c) TDTPAP for iodine adsorption by vapor sublimation.

by vapor sublimation.

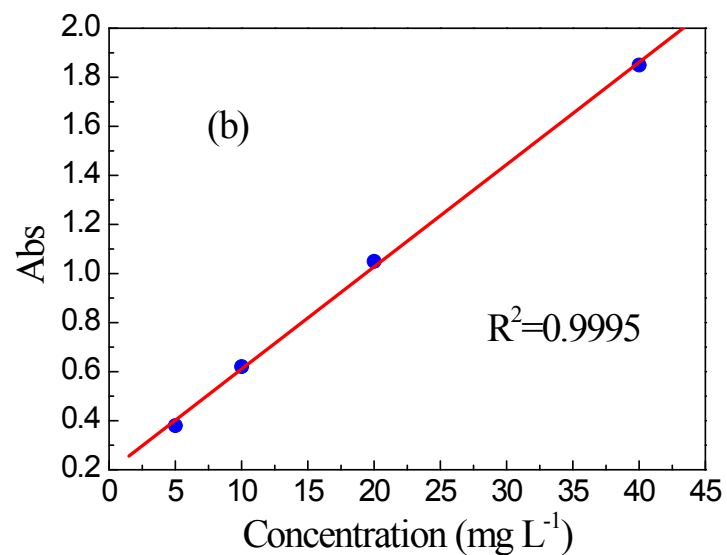
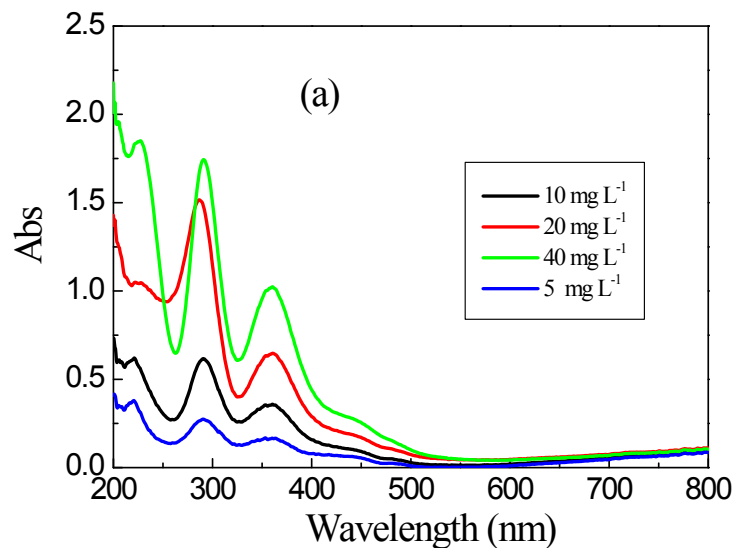


**Fig. S18.** (a) Calibration plot of standard iodine by UV-Vis spectra in cyclohexane solution. (b) The fitting of Abs value vs concentration of I<sub>2</sub> with the relatively good linearity satisfies Lambert-Beer Law.



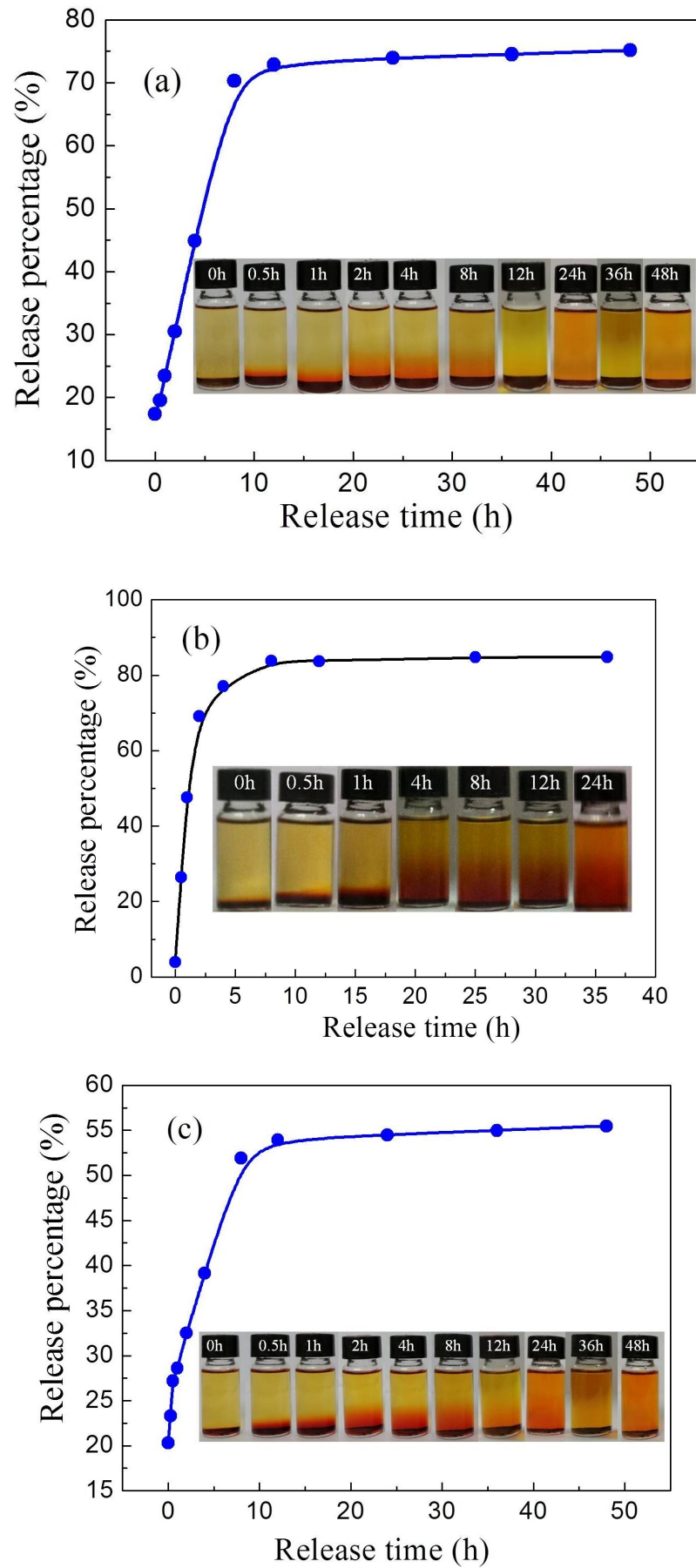


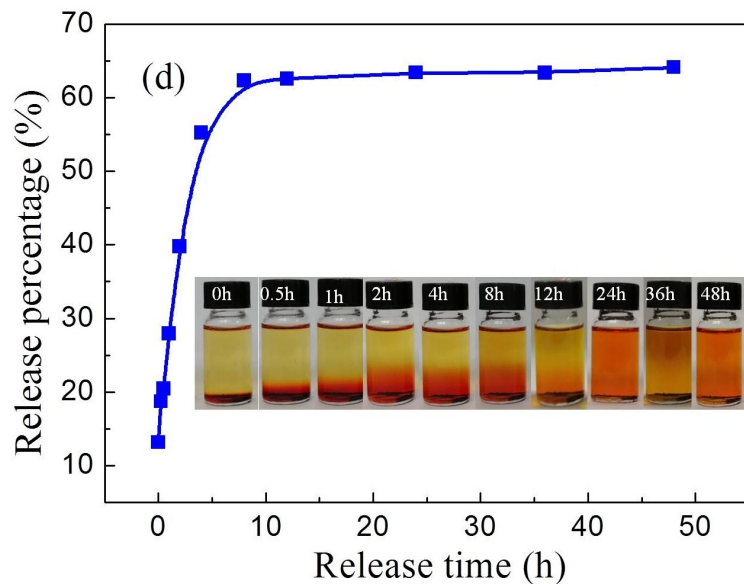
**Fig. S19.** Kinetic studies of iodine adsorption by (a) TDP ( $I_2$ - cyclohexane 100 mg  $mL^{-1}$ , 5 mL; 20 mg), (b) PCPP ( $I_2$ - cyclohexane 300 mg  $mL^{-1}$ , 5 mL; 20 mg), (c) TTPDP ( $I_2$ -cyclohexane 300 mg  $mL^{-1}$ , 5 mL; 20 mg), and (d) TDTPAP ( $I_2$ -cyclohexane 100 mg  $mL^{-1}$ , 5 mL; 20 mg) in cyclohexane solutions. Inserts: Photographs showing the color change of  $I_2$  enrichment progress.



**Fig. S20.** (a) Calibration plot of standard iodine by UV-Vis spectra in ethanol solution.

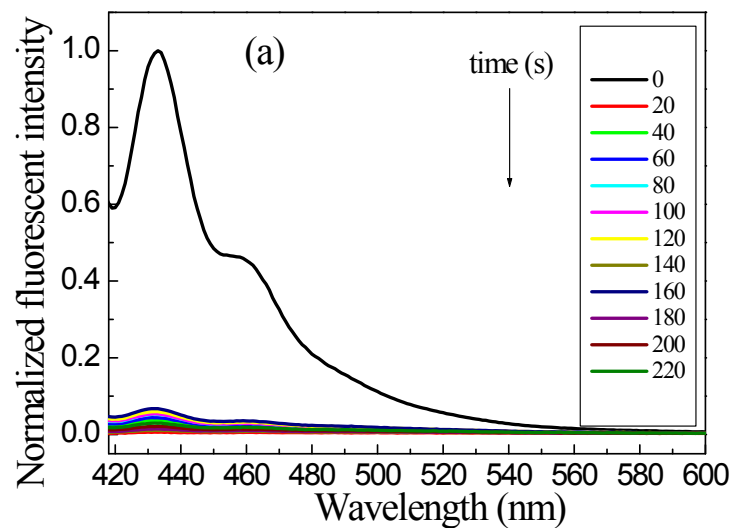
(b) The fitting of Abs value vs concentration of I<sub>2</sub> with the relatively good linearity satisfies Lambert-Beer Law.

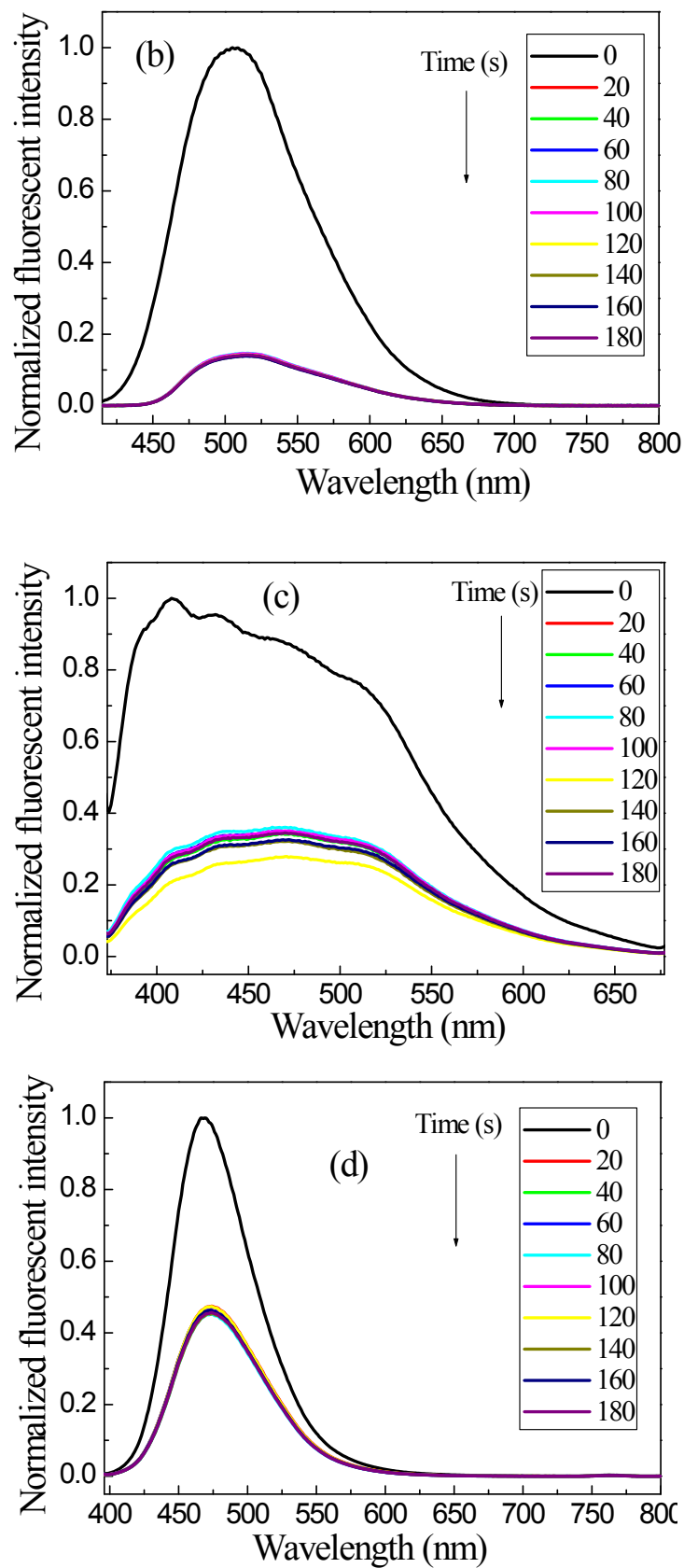




**Fig. S21.** The delivery curves of  $I_2$  from the loaded CMPs in 10 mL of EtOH.

Insert: Photographs showing progress of the iodine release from CMPs PCPP, when the containing iodine CMP networks were immersed in ethanol. (a) TDP, (b) PCPP, (c) TTPDP, and (d) TDTPAP.





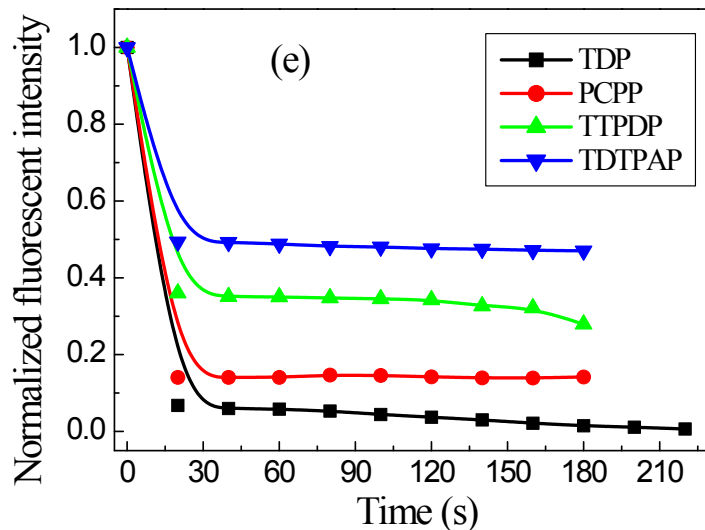


**Fig. S22.** Fluorescence spectral changes of (a) TDP in DMF dispersions upon addition of  $I_2$  ( $1.0 \times 10^{-4}$  mol L $^{-1}$ ,  $\lambda_{ex}=400$  nm), (b) PCPP in DMF dispersions upon addition of  $I_2$  ( $5.0 \times 10^{-4}$  mol L $^{-1}$ ,  $\lambda_{ex}=400$  nm). (c) TTPDP in DMF dispersions upon addition of  $I_2$  ( $2.5 \times 10^{-4}$  mol L $^{-1}$ ,  $\lambda_{ex}=380$  nm). (d) DOX dispersions upon addition of  $I_2$  ( $5.0 \times 10^{-4}$  mol L $^{-1}$ ,  $\lambda_{ex}=350$  nm) for different periods of time. (e) The curves are the evolution of maximum fluorescence intensity as a function of time.

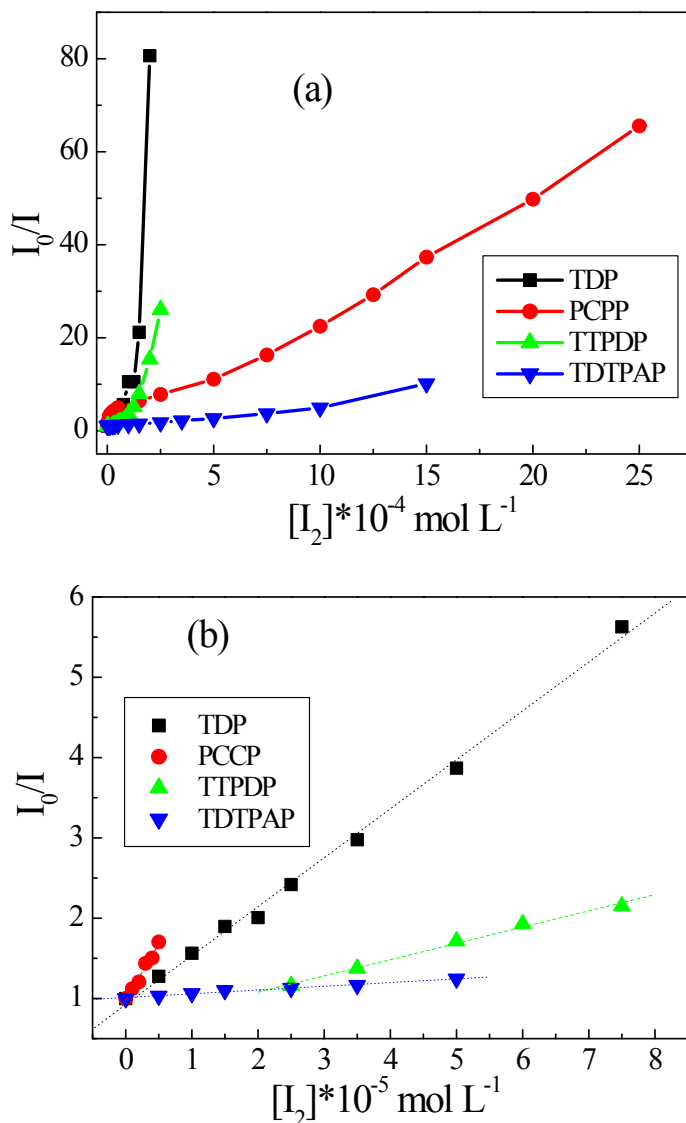


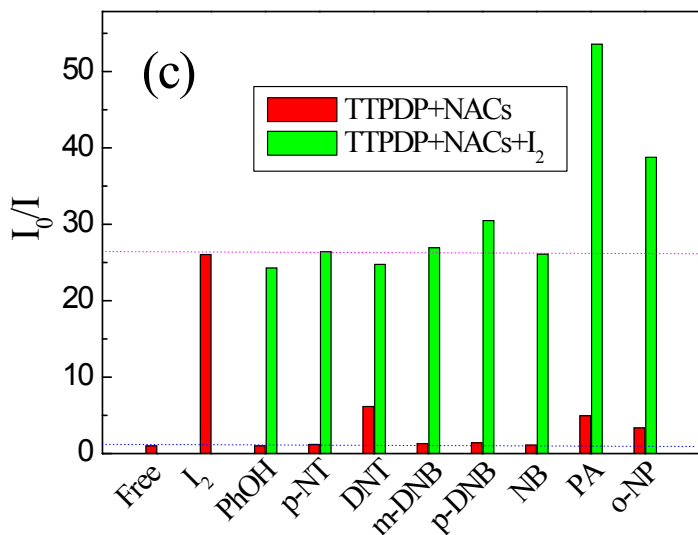
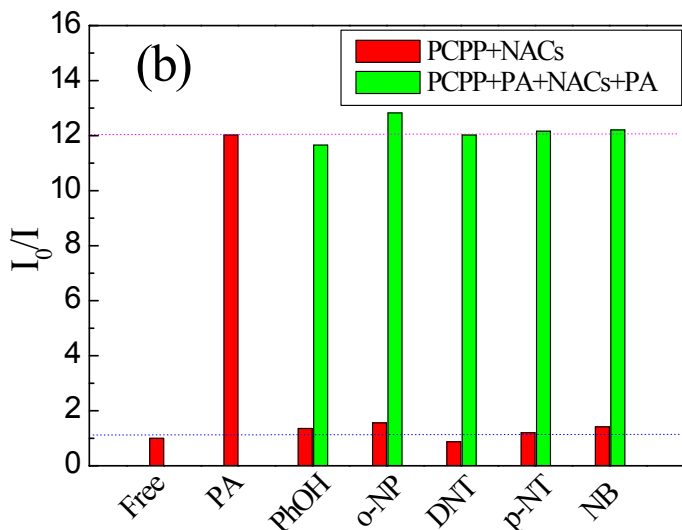
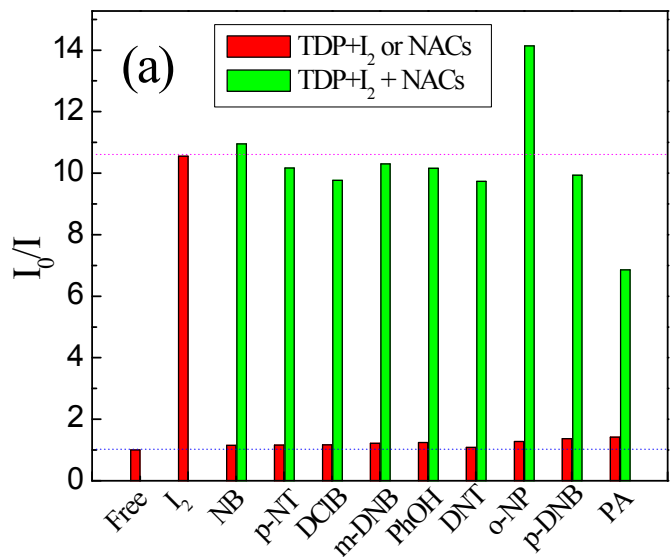
**Fig. S23.** (a) The curves are the evolution of  $I_0/I$  at maximum fluorescence intensity as a function of iodine concentrations. (b) The plots of  $I_0/I$  against  $I_2$  concentrations. Polymer concentrations: 1.0 mg mL<sup>-1</sup>; TDP (black ■, in DMF,  $\lambda_{\text{ex}}=400$  nm), PCPP (red ●, in DMF,  $\lambda_{\text{ex}}=400$  nm), (c) TTPDP (green ▲, in DMF,  $\lambda_{\text{ex}}=350$  nm), and (d) TDTPAP (blue ▼, in DOX,  $\lambda_{\text{ex}}=380$  nm).

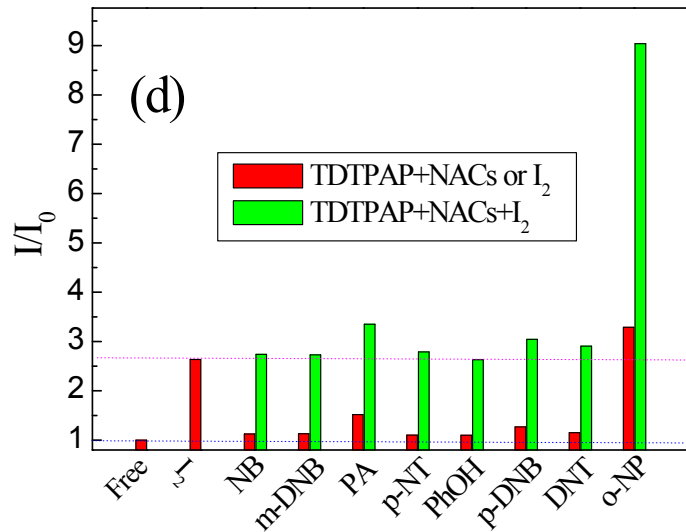
**Table S4.** The equation of  $I_0/I$  of CMPs to the concentration of  $I_2$  for suspension in DMF (TDP, PCPP, and TDTPAP) and DOX (TTPDP).

analyte	CMPs	The equation	Regression coefficient (R)	The concentration range of $I_2$ (mol L <sup>-1</sup> )	detection limit (mol L <sup>-1</sup> )
$I_2$	TDP	$I_0/I=0.9238+6.10\times10^4[I_2]$	0.9981	0 to $7.5\times10^{-5}$	$2.46\times10^{-12}$
$I_2$	PCPP	$I_0/I=0.979+1.40\times10^5[I_2]$	0.9908	0 to $5.0\times10^{-6}$	$3.14\times10^{-13}$
$I_2$	TTPDP	$I_0/I=0.6749+2.02\times10^4[I_2]$	0.9965	$2.5\times10^{-5}$ to $7.5\times10^{-5}$	$2.25\times10^{-12}$
$I_2$	TDTPA	$I_0/I=1.012+4.65\times10^3[I_2]$	0.9981	0 to $5.0\times10^{-5}$	$3.25\times10^{-10}$
P					

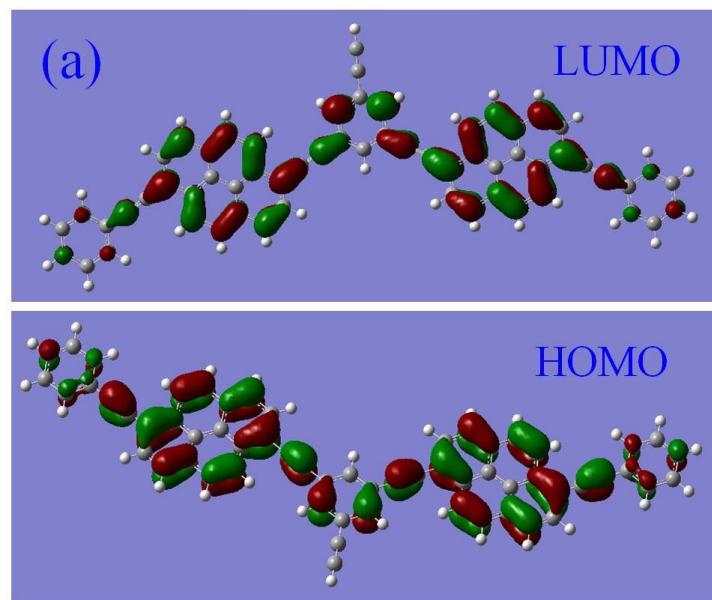
**Table S 5.** Summary of surface area and  $K_{sv}$  and LODs of POPs for fluorescence sensing to iodine

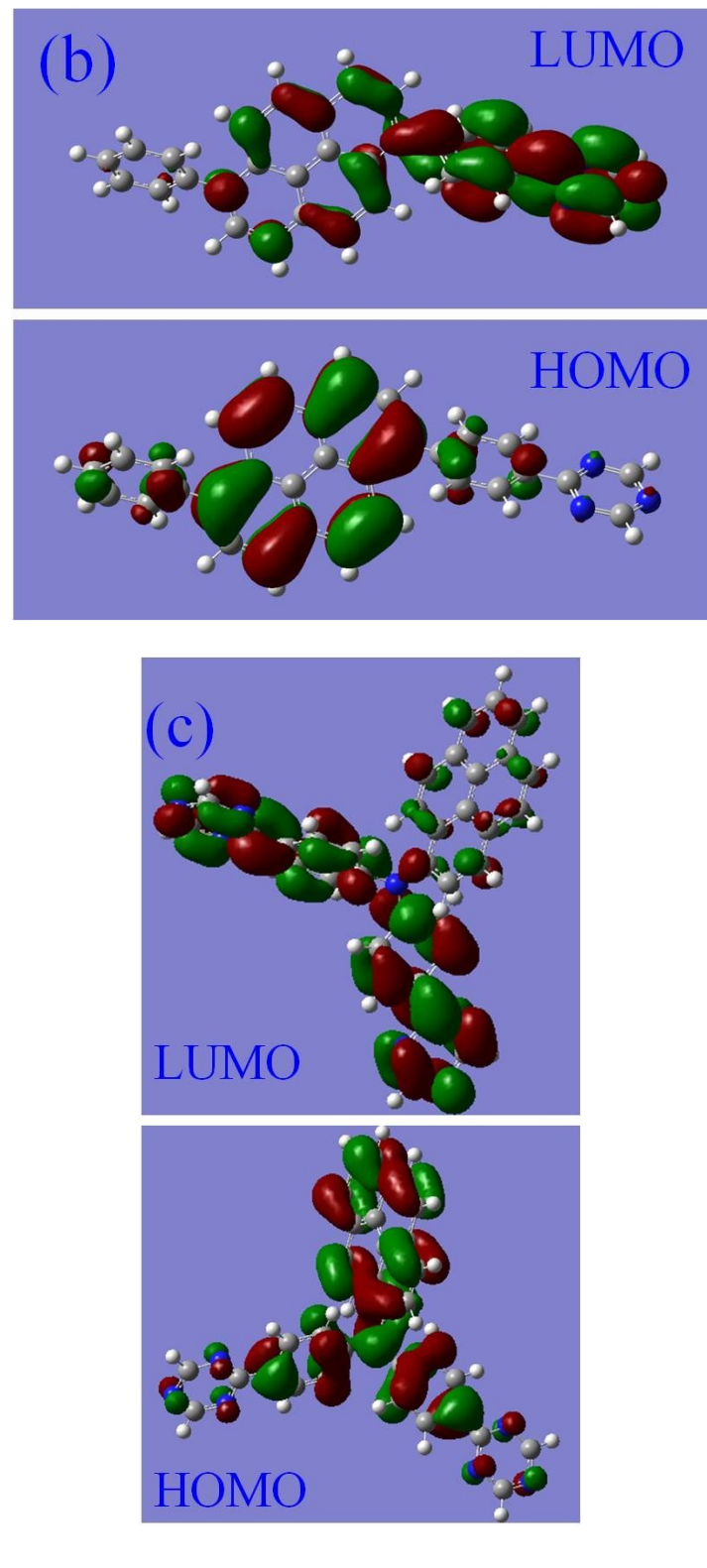
Sample	BET ( $m^2 g^{-1}$ )	$K_{sv}$ ( $L mol^{-1}$ )	LOD ( $mol L^{-1}$ )	Ref
TTPA,	308	$2.38 \times 10^4$ ,	$3.22 \times 10^{-11}$	<i>Micropor. Mesopor. Mat.</i> 273
TTDATA,	491	$4.33 \times 10^2$ ,	-	(2019) 163–170
TTMDATA	456	$7.31 \times 10^2$	-	
TS-TAD	828	$5.76 \times 10^3$	$1.56 \times 10^{-9}$	<i>Eur. Polym. J.</i>
TS-TADP	783	$5.59 \times 10^3$	$8.05 \times 10^{-11}$	115 (2019) 37–44
Cz-TPM	713.2	2372( $I^-$ )	-	<i>ACS Appl. Mater. Interfaces</i>
				2017, 9 (25), 21438–21446
PTThP-2	370.8,	$1.99 \times 10^3$ ,	$7.54 \times 10^{-8}$ ,	<i>J. Polym. Res.</i> 2019, 26: 113–
PTThP-3	748.2	$5.09 \times 10^3$	$2.95 \times 10^{-8}$	122.
TTTAT,	564.8,	$1.53 \times 10^5$ ,	$2.98 \times 10^{-12}$ ,	<i>Micropor. Mesopor. Mat.</i> 2019,
TTDAT	44.1	$9.07 \times 10^4$	$2.96 \times 10^{-13}$	284, 468–475
TDTAPAPz	4.19	$3.76 \times 10^3$	$2.47 \times 10^{-11}$	<i>Environ. Sci. Pollut. Res.</i>
TTDPz	4.41	$1.10 \times 10^3$	$1.36 \times 10^{-10}$	31 (2019) 1614–7499
TDP	261.9	$6.10 \times 10^4$	$2.46 \times 10^{-12}$	<i>This work.</i>
PCPP	43.0	$1.40 \times 10^5$	$3.14 \times 10^{-13}$	
TTPDP	187.5	$2.02 \times 10^4$	$2.25 \times 10^{-12}$	
TDTAPAP	695.2	$4.65 \times 10^3$	$3.25 \times 10^{-10}$	





**Fig. S24.** Selectivity and competition of CMPs in DMF or DOX solution ( $1.0 \text{ mg mL}^{-1}$ ) in the absence and presence of NACs and  $I_2$ , PA, respectively. (a) TDP ( $I_2$  in DMF,  $1.5 \times 10^{-4} \text{ mol L}^{-1}$ ,  $\lambda_{\text{ex}}=400 \text{ nm}$ ), (b) PCPP (PA in DMF,  $1.0 \times 10^{-4} \text{ mol L}^{-1}$ ,  $\lambda_{\text{ex}}=400 \text{ nm}$ ), (c) TTPDP ( $I_2$  in DMF,  $2.5 \times 10^{-4} \text{ mol L}^{-1}$ ,  $\lambda_{\text{ex}}=350 \text{ nm}$ ), (d) TDTPAP ( $I_2$  in DOX,  $5.0 \times 10^{-4} \text{ mol L}^{-1}$ ,  $\lambda_{\text{ex}}=380 \text{ nm}$ ).





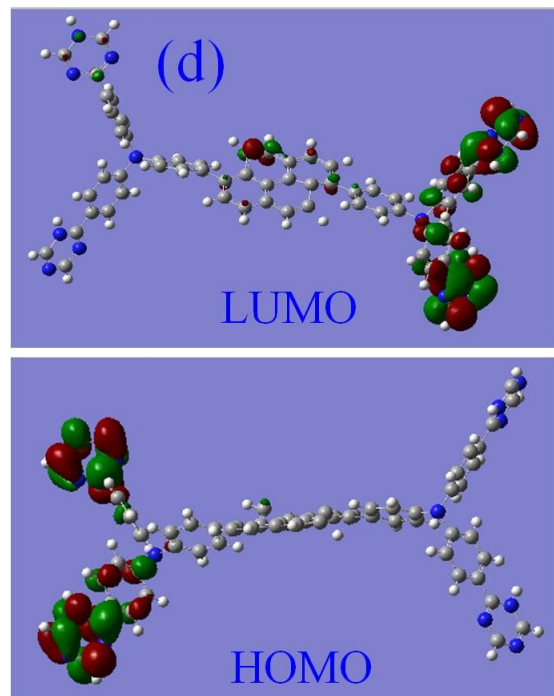


**Fig. S25.** HOMO and LUMO orbital diagrams of CMPs (a) TDP, (b) PCPP, (c) TDTPAP, and (d) TTPDP. The molecular orbital calculations were performed with the Gaussian 09 D 0.1 program at the B3LYP/6-31G (d) level.